

The Dynamic Likelihood Filter

J. M. Restrepo*

Department of Mathematics & College of Earth Ocean and Atmospheric Sciences, Oregon State University

*Correspondence to: Department of Mathematics, Oregon State University, Corvallis OR 97330

A Bayesian data assimilation scheme is formulated for advection-dominated or hyperbolic evolutionary problems, and observations. The method is referred to as the dynamic likelihood filter because it exploits the model physics to dynamically update the likelihood with the aim of making better use of low uncertainty sparse observations. The filter is applied to a problem with linear dynamics and Gaussian statistics, and compared to the exact estimate, a model outcome, and the Kalman filter estimate. Its estimates are shown to be superior to the model outcomes and the Kalman estimate, when the observation system is sparse. The added computational expense of the method is linear in the number of observations and thus computationally efficient, suggesting that the method is practical even if the space dimensions of the physical problem are large.

Key Words: data assimilation; dynamic likelihood; kalman filter; forecasting; wave equation; hyperbolic equation.

Received ...

1. Introduction

Data assimilation is a Bayesian framework for combining models and observations, taking into account their respective inherent uncertainties. These uncertainties are often represented by statistical processes. Among other things, model uncertainties might represent unresolved, or poorly understood physics, or poorly constrained parameters, or uncertainties in boundary conditions and initial conditions. Observation uncertainties derive from measurement errors and errors associated with projecting the observations onto model space. The goal of data assimilation is to produce estimates of moments of the posterior distribution of the state vector, conditioned on observations.

Whether the problem is time-dependent or not, under linear dynamics and when the noise processes are Gaussian, the minimizer of the posterior distribution covariance can be found via least squares. For time-independent problems an efficient computational optimization strategy, based upon variational extremization, is known as 3DVAR (see Hamill and Snyder (2000)). For time dependent problems a smoother estimate can be found via 4DVAR (see Courtier *et al.* (1993) , and Lorenc and Hammon (1988) and references contained therein), or via the sequential Kalman smoother (see Wunsch (1996)).

Geophysical processes are seldom linear. There are data assimilation methods that can handle nonlinear/non-Gaussian problems, however, none seems to be capable of handling the inherently large number of degrees of freedom of evolution problems that can be captured by partial differential equations at reasonable resolutions, *e.g.*, a weather model. Among the methods capable of handling the nonlinear/non-Gaussian cases we could mention sampling-based methods, such as the Path Integral Monte Carlo of Alexander *et al.* (2005) and Restrepo (2008), and the Langevin sampler (*cf.*, Stuart *et al.* (2004));

a host of particle filter methods (*cf.*, Kim *et al.* (2003), and Chorin *et al.* (2010) and references contained therein); variance-minimizing methods (see Kushner (1962), Kushner (1967b), Kushner (1967a)); entropic methods, such as the Mean Field Variational Method of Eyink *et al.* (2004). Ad-hoc approaches that yield reasonable outcomes in high dimensional weakly nonlinear problems, with strong statistical unimodality, are also known. Of note is the ensemble Kalman Filter (enKF, see Evensen (2003, 2004)). Its ad-hoc nature rests upon the fact that the method uses nonlinear dynamics in the forecast, and Gaussian assumptions in the analysis, *i.e.*, the stage in which data and model outcomes are blended. The method exploits ensemble ideas in order to estimate covariances, hence, it is very efficient in computational storage requirements. The method is also attractive because it easily handles dynamic problems that present themselves in the form of legacy code.

Filtering techniques have been proposed that make use of some form of nudging to improve the stability of the filtering method in the presence of nonlinearity, and/or when there are large discrepancies in the relative uncertainty in model outcomes and measurements. The earliest strategies achieve nudging via empirical dynamic relaxation (see Hoke and Anthes (1976), for example). More modern strategies that are worthy of mention: the equivalent-weights particle filter Ades and VanLeeuwen (2015), and the near-optimal guided particle filter of Weare and Vanden-Eijnden (2013). A different approach, a predictor-corrector method, was proposed recently by Rosenthal *et al.* (2016), is called *displacement assimilation*. In this method kinematic flow constraints are used in the filtering of data and model outcomes. Specifically, the estimation process is constrained using the divergence-free condition, a fundamental property of the velocity field underlying the advection/dispersion

of a tracer in an incompressible flow. The incompressibility condition is imposed on the filtering forecast of the time-dependent problem via a correction to the local metric of space/time and thus adds to the forecast and analysis stage, another stage that makes a displacement correction. Similar methodologies have been proposed, for example, by Ravela and collaborators (*cf.*, Ravela (2012)), and Nehrkorn *et al.* (2015).

A data assimilation strategy based on filtering is proposed that is tailored to evolutionary problems dominated by advective processes, in situations where low uncertainty but sparse observations are available. Sparsity in the observation system is the norm, rather than the exception, in spatially extended, temporal forecasting and analyses. The proposed method is called the *dynamic likelihood filter* (DLF) because it uses the dynamics of the physical problem to update in time the likelihood probability density function. By doing so a sparse network of low uncertainty observations will be “nudged” in order to have a greater impact on the posterior distribution of the state vector, conditioned on observations. The DLF can be used in forecasting, since it can project present and past observations into the future in order to retain the capability of making Bayesian estimates. Two versions of the methodology are foreseen: the case where the observation system is stationary, and when it has its own dynamic. The stationary case will be addressed in this study, applied to the simplest of physical models. The moving observation system, to be addressed separately, leads to a variant of an assimilation scheme called Lagrangian data assimilation (see Kuznetsov *et al.* (2003), for example, Restrepo (2008) and Krause and Restrepo (2009), for issues addressing non-Gaussianity).

2. Statement of the Problem

We consider the problem of generating moment histories, over a time spanning $t \in [0, t_f]$, of the \mathbb{R}^N random state vector $U(t)$, conditioned on noisy observations $Y(t_m) \in \mathbb{R}^K$, $m = 1, 2, \dots, M$. The time t_f , for the DLF, may be set in the future. The measurement or filtering times t_m do not extend beyond the present time t_p . The simplest possible linear dynamics, with uncertainties represented by normally-distributed noise, will be pursued here.

For notational convenience the Kroneker delta function will be redefined as follows:

$$\delta_{n,m} := \begin{cases} 1, & \text{if } t_n = t_m, \\ 0, & \text{otherwise.} \end{cases}$$

2.1. The Dynamics

It is assumed that $U(t)$ is a finite-dimensional vector, with entries $U_\ell(t) = u(x_\ell, t)$, $\ell = 1, 2, \dots, N$. The coordinates $\{x_\ell\}_{\ell=1}^N := X$ are fixed, distinct, and equi-distant (though they do not have to be so). The X coordinates will be denoted the *state coordinates*. The wave $u(x, t)$ obeys

$$\begin{aligned} u_t - C(x, t)u_x &= F(x, t), \quad t > 0, x \in [0, L], \\ \langle u(0, t) \rangle &= \langle u(L, t) \rangle, \quad t \geq 0, \\ u(x, 0) &= \mathcal{U}(x), \quad x \in [0, L], \end{aligned} \quad (1)$$

the subscripts x and t connote partial differentiation with respect to these variables, the $\langle \cdot \rangle$ is the ensemble-average operator. It will be further assumed that $\langle F \rangle$ and $\langle \mathcal{U} \rangle$ are periodic on the interval L . The source/sink or *forcing* F as well as the phase speed $C(x, t)$ are noisy, with known, zero-mean, additive noise.

The solution of (1) for a finite set of solutions following characteristics can be found as follows: Let the vector $\Phi(t)$ be

such that $\Phi_\ell(0) = \mathcal{U}(x_\ell)$. For $\ell = 1, 2, \dots, N$,

$$\begin{aligned} \frac{d\Phi_\ell}{dt} &= F_\ell(x, t), \quad t > 0, \\ \Phi_\ell(0) &= \mathcal{U}(x_\ell). \end{aligned} \quad (2)$$

The initial condition $\mathcal{U}(x_\ell)$ has a known probability density function (pdf), and

$$F_\ell dt = f(x, t)dt + A_\ell(t)dW_\ell^{(f)}(t),$$

where $\langle F_\ell(x, t) \rangle = f(x, t)$. The noise in the forcing is captured by the incremental zero-mean Wiener process $dW_\ell^{(f)}(t) \in \mathbb{R}^N$, with known variance $A(t) \in \mathbb{R}^N$. The solution of (2) requires the solution of the equation for the characteristics, namely,

$$\begin{aligned} \frac{dx_\ell(t)}{dt} &= C_\ell(x, t), \quad t > 0, \\ x_\ell(0) &= x_\ell, \quad \ell = 1, 2, \dots, N, \end{aligned} \quad (3)$$

where

$$C_\ell(x, t) dt = c(x, t)dt + B_\ell(t)dW_\ell^{(c)},$$

with $c(x, t) := \langle C \rangle(x, t)$. The second term in the characteristic equation represents uncertainties in the wave speed. These uncertainties are assumed to be well captured by the (zero mean) Wiener incremental process $dW_\ell^{(c)}(t) \in \mathbb{R}^N$, with known variance $B(t) \in \mathbb{R}^N$.

The solution of (1)-(3) will be referred to as the *Exact* solution. Ensemble members we denote as *Truth* will be constructed, using the exact solutions. The Truth estimate is an ensemble member of the exact solution set, linearly interpolated onto the grid X , evaluated at discrete times $t_n = n \Delta t$, $n = 0, 1, 2, \dots, N_f$, where Δt is constant.

In geoscience applications, evolutionary models for physical phenomena commonly present themselves in the form of a computer code, for the discrete-in-time and -in-space approximation of a model for the physics in question. The *Model* outcome $V_n \in \mathbb{R}^N$ will be a discretized approximation of the vector $U(t)$ representing approximations of the solution on X of (1) at times t_n . The discretization generates truncation errors which manifest themselves as biasing errors. This source of error will not be addressed here. There are errors and uncertainties associated with how well the unresolved physics of the process is captured. In hyperbolic problems it is typical to have uncertainties in the forcing *i.e.*, sources/sinks, as well as in the wave speed.

The model is assumed to be of the form

$$\sqrt{\Delta t} \Delta w = -V_n + L_n V_{n-1} + \Delta t f_{n-1}, \quad n = 1, 2, \dots, N_f, \quad (4)$$

where V_n is periodic, *e.g.*, $\langle V_n^0 \rangle = \langle V_n^N \rangle$, and the periodic initial condition for the vector is known: $V_0^\ell := \mathcal{U}(x_\ell)$. Samples of the incremental noise Δw come from a normal variate (the prior π_n is a normal variate). The model noise variance $Q_n = \Delta t \langle w_n w_n^\top \rangle \delta_{n,n'}$ is assumed known (that the noise is uncorrelated is not a requirement in what follows).

At discrete times, *Observations* are available:

$$\epsilon(t_m) = Y(t_m) - H(t_m)V(t_m), \quad m = 1, \dots, M. \quad (5)$$

The observation errors $\epsilon(t_m)$ have a known pdf. The distribution of ϵ_m is given by the likelihood $\pi_m(Y_m|V_m)$. A linear observation network is considered. The observation network will be assumed to coincide with a subset of or with all locations specified by X . The observation matrices, $H(t_m) : \mathbb{R}^N \rightarrow \mathbb{R}^K$. Without loss of generality it will be assumed that observations are taken at discrete intervals $t_m \in [0, t_p]$. Further, the observation or *filtering times*

are taken to be equally spaced, $t_m = m \delta t$, $m = 1, 2, \dots, M$, and $\delta t \geq \Delta t$, fixed. It is assumed that the model and observation noise processes are uncorrelated. The observation errors are normally distributed and have variance

$$R_m := \langle \epsilon_m \epsilon_m^\top \rangle \delta_{m,m'}. \quad (6)$$

3. Data Assimilation via Filtering

The data assimilation problem can be stated as follows: *Find an estimate of the ensemble mean and the uncertainty of the random vector $U(t)$, at times t_n , $n = 0, 1, \dots, N_f$, given a set of random observations $Y(t_m)$, $m = 1, 2, \dots, M$.*

The estimate will be found by minimizing the trace of the posterior covariance of the conditional probability

$$\pi(V|Y) := \pi(Y|V) \prod_{n=0}^{N_f} \pi_n. \quad (7)$$

The prior, π_n , informed by model outcomes, depends on V_i , $i = n, n-1, \dots, 0$, and is independent of the likelihood. The likelihood, informed by observations, is

$$\pi(Y|V) := \prod_{m=1}^M \pi_m(Y_m|V_m). \quad (8)$$

The pdfs π_n and $\pi(Y|V)$ are known and will be described below.

For linear/Gaussian problems obtaining the posterior mean and covariance allows us to fully characterize the posterior distribution. A well-known algorithm for finding the Kalman smoother estimator is the RTS algorithm (the algorithm is described in Wunsch (1996)). It is based on the Kalman Filter (see Jazwinski (1970)).

Sparsity of observations, *i.e.*, $K \ll N$, and low uncertainties in them, as compared to the large dimensions and higher modeling uncertainties of phenomena captured by partial differential equations, is a realistic situation, particularly in geoscience applications. The Kalman filter will be modified in order to improve the estimate of the ensemble-averaged approximation of the wave solution, using observations made with low uncertainties by a sparsely-distributed measuring system. Sparsity in the observation network can lead to a variety of special challenges: Sparsity can lead to likelihoods that are not very informative: the posterior will be overwhelmed by the prior; if the likelihoods are extremely localized, as they would be if the measurements have low uncertainties, it is possible that the Bayesian inference problem becomes ill-posed, particularly if there are biases that are not properly accounted for. Obtaining improved estimates when observations are sparse is the central motivation for formulating the proposed assimilation scheme.

3.1. The Kalman Filter (KF)

The Kalman Filter produces a sequential estimate in two steps. In the *forecast* step the model is used to produce an initial estimate. Since the model is linear and the noise is (unbiased) normal, the mean state $\langle V \rangle_n$ is obtained from $\langle V \rangle_{n-1}$ using

$$\tilde{V} = L_{n-1} \langle V \rangle_{n-1} + \Delta t f_{n-1}, \quad n = 1, 2, \dots, N_f. \quad (9)$$

It is easy to form the equation for the evolution of the covariance $P_n = \langle e_n e_n^\top \rangle$, where $e_n := V_n - \langle V \rangle_n$:

$$\tilde{P} = L_{n-1} P_{n-1} L_{n-1}^\top + Q_{n-1}, \quad n = 1, 2, \dots, N_f. \quad (10)$$

If no observations are available at time n , the posterior is not affected by the likelihood at t_n and thus $\langle V \rangle_n = \tilde{V}$, and $P_n = \tilde{P}$.

($\langle V \rangle_0$, and P_0 are known). If, on the other hand, $t_n = t_m$, observations are available. An *analysis* step is performed, that takes in the tilde variables \tilde{V} and \tilde{P} and updates these to produce a mean and the covariance estimate. Defined for any step t_n , the analysis step consists of the update

$$\langle V \rangle_n = \tilde{V} + K_m (Y_m - H_m \tilde{V}), \quad (11)$$

$$P_n = (I_N - K_m H_m) \tilde{P}. \quad (12)$$

The second term in (11) is called the *innovation*. In (12) I_N is the N -dimensional identity matrix. The Kalman Gain is defined as

$$K_m = \tilde{P} H_m^\top [H_m \tilde{P} H_m^\top + R_m]^{-1} \delta_{n,m}. \quad (13)$$

3.2. The Dynamic Likelihood Filter (DLF)

An alternative Bayesian statement is proposed, for the posterior pdf. In the DLF the pdf, at time n , is

$$\pi(Y|V)_n := \pi_m(\{\mathcal{H}Y_m\}_{t_m \leq t_n} | V_n), \quad (14)$$

where the data Y_m , for all measuring times t_m less than or equal to time t_n , can influence the likelihood at time t_n (*cf.*, to (8)). The linear operator \mathcal{H} projects data from the past to the present and further, maps it onto the state coordinates, X .

In other words, the observations will not only inform the likelihood at time t_m , but will do so at subsequent times. The observation data and its uncertainty are propagated forward in time, from t_m to t_n . The forward-propagated data is used, provided that their inherent uncertainty has not grown (degraded) beyond some set threshold. In doing so high quality but sparse resources of information are exploited more thoroughly. There is good reason to think that in highly local problems in which information travels at finite speeds, this strategy may deliver improved estimates, particularly of phase-sensitive information as well as structure. Clearly, if the data is neither sparse or is endowed with high uncertainties, compared to the uncertainties in the model, the methodology would not be recommended.

One can envision two ways of using the likelihood dynamically: one is when the observation network is stationary. The other modality would correspond to when the observation network moves in space and time. This latter case corresponds to a type of Lagrangian data assimilation (*cf.*, Kuznetsov *et al.* (2003)), and will be developed in detail in a separate paper.

3.2.1. Dynamic Likelihood on a Fixed Observation System

What is meant by a stationary observation network is that the observations take place at prescribed locations $Z \subseteq X$, for all t , where $\dim(Z) = K$. The *observation coordinates* Z are taken to coincide with components of the lattice X in order to avoid the complications that come with the addition of a Gauss-Markov interpolation between the state coordinates and the observation coordinates. (A moving observation system, on the other hand, will have $Z = Z(t)$).

Observations from the fixed observation system will be used at times t_m when they become available, as well as at subsequent times, once their phase and uncertainty is updated. Using the known estimate for the mean speed $c(x, t) = \langle C(x, t) \rangle$, the observation phase is updated by computing the wave characteristics emanating from the location of the observation. The semi-Lagrangian approximation for the virtual dynamics of observational data is used to propagate the observations into future fixed times, the method makes use of the semi-Lagrangian approximation Staniforth and Coté (1991) to solutions to data that

evolves according to $Y_t - c(x, t)Y_x = 0$, on the time grid. That is,

$$\begin{aligned}\zeta_{n+1} &= \Delta t c(\zeta_n, t_n) + \zeta_n, \quad t_n \geq t_m, \\ Y(\zeta_{n+1}, t_{n+1}) &= Y(\zeta_n, t_n),\end{aligned}\quad (15)$$

with $\zeta_0 = H(t_m)X$, and $Y(\zeta_0, t_m) = Y_m$.

The variance associated with the measurements at t_m is known and equal to R_m , but it cannot be expected to remain the same, for $t_n > t_m$. Since the inherent dynamics of the problem are being used to project forward in time, it may be argued that the manner in which the uncertainty of these projected observations change is dictated by the uncertainty in the dynamics. If this argument is reasonable

$$R_m^{n+1} = A_n(t)[A_n(t)]^\top \Delta t + R^n, \quad t_n \geq t_m, \quad (16)$$

where $R_m^m = R_m$.

The decision on how this data is used must rely on sensible choices in the computation and the estimation process. It is decided that measurements propagated forward in time that reach some threshold of uncertainty should cease contributing to the likelihood. Presuming the data has lower uncertainty than the model, a reasonable uncertainty threshold for measurements propagated forward in time, is that their variance not exceed the variance in the model in the same spatial neighborhood. Using (16) it is easy in fact to estimate the total time beyond t_m that data is viable, given this threshold or some other criteria.

The dimension of the viable observations can exceed N . Computationally, this may lead to having to address numerical stability issues differently when the system goes from under determined to an overdetermined system. Moreover, the Kalman strategy presumes that a single innovation vector be used to update the forecast which in turn means addressing complexities in the observation matrix. In what follows choices are made to keep the number of observations used at any given time t_n bounded by N . Furthermore, the propagated observations are ordered by the norm of their uncertainty and preference will be given to observations with lower uncertainty.

3.2.2. When Measurements Relate to the State via a Linear Transformation

For the linear dynamics the Kalman Filter is still a viable estimation strategy. In the DLF, as applied to linear/Gaussian problems, the forecast stage of the Kalman Filter remains the same. What changes is the analysis stage. The correction stage of the algorithm will be referred to as the multi-analysis. It entails building an alternative innovation vector and a Kalman gain.

In the usual Kalman Filter, an ‘‘observation’’ matrix projects the state vector onto the space of measurements and their uncertainties. Here, the ‘‘reverse’’ case is developed, wherein a matrix projects the measurements and their errors onto the state vector.

The crux is to develop the sequential estimation when the observation matrix \mathcal{H} appears thusly:

$$\mathcal{H}_m^n Y_m^n = V_n + \mathcal{H}_m^n \epsilon_m^n, \quad (17)$$

at time $t_n \geq t_m$. Here ϵ_m^n is equal to ϵ_m . The multi-analysis stage is now

$$\langle V \rangle_n = \tilde{V} + \mathcal{K}_m(\mathcal{H}_m Y_m - \tilde{V})\delta_{m,n}. \quad (18)$$

Since $P_n = \langle (\langle V_n - \langle V \rangle_n)(\langle V_n - \langle V \rangle_n)^\top \rangle$, it is then possible to express the covariance, using (17), as

$$P_m = \langle (I - \mathcal{K}_m)\tilde{P}(I - \mathcal{K}_m)^\top \rangle + \mathcal{K}_m \mathcal{H}_m R_m \mathcal{H}_m^\top \mathcal{K}_m^\top. \quad (19)$$

The trace of the covariance is

$$\text{Tr}[P_m] = \text{Tr}[\tilde{P}] - 2\text{Tr}[\mathcal{K}_m \tilde{P}] + \text{Tr}[\mathcal{K}_m(\tilde{P} + \mathcal{H}_m R_m \mathcal{H}_m^\top)\mathcal{K}_m^\top].$$

Differentiating with respect to \mathcal{K}_m and setting the derivative to zero, one finds the extremizer of the trace is

$$\mathcal{K}_m = \tilde{P}(\tilde{P} + \mathcal{H}_m R_m \mathcal{H}_m^\top)^{-1} \delta_{m,n}. \quad (20)$$

Using (20) back in (19) we find the update to the covariance is

$$P_n = (I - \delta_{m,n} \mathcal{K}_m)\tilde{P}. \quad (21)$$

3.3. Formulating a Low Uncertainty Likelihood

The expressions for the Kalman Gain (20) and the uncertainty (21), for this linear-Gaussian version of the DLF, are purely formal at this point. In the dynamic likelihood assimilation it will be generally the case that several observations will have a bearing on a single state variable entry. If the measurements are very sparse in space, a simple option is to use

$$\mathcal{H}_m^n Y_m^n(x_\ell) := \mathcal{I} \mathcal{J} Y_m^n(x_j(t_n)) = \mathcal{I} \mathcal{Y}(x_\ell),$$

The *projection operator* \mathcal{J} is defined as

$$\mathcal{J} := [\delta_{\ell,j}^n (1 - b_j^n) + \delta_{\ell-1,j}^n b_j^n], \quad (22)$$

where $b_j^n = b_0 \text{rem}(x_j(t_n), \Delta x)$, the remainder, and b_0 is a normalization constant. In (22) the Kronecker delta symbols are used in the traditional sense. (The projection operator \mathcal{J} must be modified to take into account boundary conditions). The matrices project the updated datum at position x_j onto the fixed grid x_ℓ by weighting the data according to the proximity of x_j to the grid on which x_ℓ belongs. A simpler alternative is to set b_j^n to zero. This latter option will be used in the example calculations that appear later on.

With regard to choosing which measurements to use in the filtering stage, when there are choices to be made, the following procedure is suggested: at any given time, measured or updated measurements are ordered in increasing size in their associated uncertainty. The rank-ordering operator accomplishes this. Observations available presently or propagated from the past may be available to perform a multi-analysis and may share the same projected location x_ℓ . The *rank-ordering operator* \mathcal{I} assigns a single datum to x_ℓ , among those that are available. The datum will have the lowest uncertainty among all of the data that can inform the likelihood at location x_ℓ , from the present or from the past. Let $\mathcal{I}_k = D_{k+1} + E_{k+1}$, $k = 0, 1, \dots$, then

$$\mathcal{I}_0 \mathcal{Y} = D_1 \mathcal{Y} + E_1 [D_2 \mathcal{Y} + E_2 [D_3 \mathcal{Y} + E_3 [D_4 \mathcal{Y} + \dots]]], \quad (23)$$

i.e., the rank-ordering operator is applied recursively.

An example illustrates the rank-ordering operator. Suppose there are 11 state stations. The goal is to construct the innovation vector at some time step n . Figure 1 schematically portrays the observations and/or their projected values. It will be assumed that the uncertainty associated with measurements grows linearly in time. The measurements, or their dynamic updates, have been projected already onto the state stations. Figure 1 displays the set of observations and/or their projected values, at time n . The data has been arranged, from left to right, in order of increasing uncertainty. For this example the matrices are

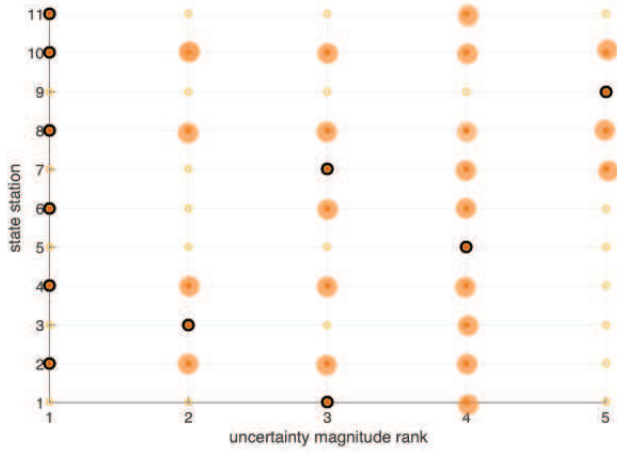


Figure 1. Rank-ordering operator schematic. Measurements, projected forward or from the present, are organized from left to right in increasing uncertainty. The measurements have been already been projected onto the state stations, via the \mathcal{J} operator. The state stations are labeled 1 through 11. Available data appear as filled circles. The data that will be used in the innovation appears as dark, multi-colored filled circles. The datum with the least uncertainty at a specific state station will contribute to the innovation. In this example data manages to inform all of the stations.

$$\begin{aligned}
 D_1 = \delta_{i,j} & \begin{bmatrix} 0 \\ 1 \\ 0 \\ 1 \\ 0 \\ 1 \\ 0 \\ 0 \\ 1 \\ 1 \\ 1 \end{bmatrix}, D_2 = \delta_{i,j} \begin{bmatrix} 0 \\ 1 \\ 1 \\ 0 \\ 0 \\ 0 \\ 1 \\ 0 \\ 1 \\ 1 \\ 0 \end{bmatrix}, D_3 = \delta_{i,j} \begin{bmatrix} 1 \\ 1 \\ 0 \\ 1 \\ 0 \\ 1 \\ 1 \\ 0 \\ 1 \\ 1 \\ 0 \end{bmatrix}, \\
 D_4 = \delta_{i,j} & \begin{bmatrix} 1 \\ 1 \\ 1 \\ 1 \\ 1 \\ 1 \\ 1 \\ 0 \\ 1 \\ 1 \\ 1 \end{bmatrix}, D_5 = \delta_{i,j} \begin{bmatrix} 0 \\ 0 \\ 0 \\ 0 \\ 0 \\ 1 \\ 1 \\ 1 \\ 1 \\ 0 \end{bmatrix}, \quad i, j = 1, 2, \dots, nx.
 \end{aligned}$$

3.4. The Mutli-Analysis and the Kalman Gain

The multi-analysis is

$$\langle V \rangle_n = \tilde{V}_n + \mathcal{K}_n \sum_{m' \in m} (\mathcal{H}_{m'}^n Y_{m'}^n - \tilde{V}_n), \quad (24)$$

The data Y_m^n is advanced via (15), or its ensemble-forced counterpart if the physics has forcing. The uncertainty R_m^n is updated via (16) (or its forced counterpart).

To obtain an expression for the Kalman Gain, we extremize the trace of the posterior covariance, just as was done in Section 3.2.2. The result for the Kalman gain and the uncertainty, respectively, are

$$\mathcal{K}_n = \tilde{P}_n (\tilde{P}_n + \sum_{m' \in m} \mathcal{H}_{m'}^n R_{m'}^n [\mathcal{H}_{m'}^n]^\top \vartheta_{m',n})^{-1}, \quad (25)$$

where $\vartheta_{m',n}$ is the Heaviside function, and

$$P_n = (I - \mathcal{K}_n) \tilde{P}_n. \quad (26)$$

3.5. The Linear/Gaussian DLF Algorithm

The algorithm for DLF, for the linear Gaussian case, which allows the use of the Kalman filter framework, proceeds as follows: at some state time $t_n > 0$, and given that at $t = 0$ the mean of the state of the system and its uncertainty are known:

- The forecast stage is the same as the one employed in the Kalman Filter, *i.e.*, (9)-(10).
- The multi-analysis stage:
 - Observations from times $t_m < t_n$ are propagated forward up to time at t_n . The propagation is effected by using the mean eigenspeeds, along characteristics. Their uncertainties are propagated forward as well. At measuring times the uncertainties in the observations are given by the known measurement error.
 - The innovation vector is built using the projection and the uncertainty rank operators.
 - The Kalman gain is computed via (25).
 - The multi-analysis is performed using (24), yielding an estimate of the mean state.
 - The uncertainty of the state is updated via (26).
- The forecast and multi-analysis is repeated till time t_f , along the way the measurements are used in formulating the multi-analysis stage. If the presumption is that the model error is larger than the observation error, one can use an uncertainty threshold to shed measurements in the multi-analysis that, due to being propagated forward in time, have an unacceptably high uncertainty as compared to the model uncertainty at that particular time t_n .

We emphasize again, that t_f can be set into the future, the filtering takes place using the model and time-projected data.

4. Comparing the Model, the KF, and the DLF Outcomes

Comparisons will be made between the outcomes from the Lax-Friedrich calculations, which we will call the ‘‘Model’’ outcomes, and assimilation results from the Kalman Filter (KF) and the Dynamic Likelihood (Kalman) Filter (DLF). These are compared, in turn, to the Truth.

The observations are available at times t_m , on all or a portion of the state space stations X . At time t_m the measurements have fixed measurement variance R . They are the same for the Kalman and the DLF. However, in DLF the observations are used in the innovation vector at time t_m and times thereafter. For $t > t_m$ the observations are updated in space and time as are their uncertainties. Their impact on the estimate at times t_n and stations X is found via the multi-analysis.

The aims of the calculations are to show that the mean delivered by data assimilation is superior to the model outcome; and to show that when the observation system is sparse, the DLF yields outcomes that are better than KF with regard to phase, uncertainty, and in many instances, in qualitative terms.

The two parameters in the examples will be the frequency of spatial sampling ξ , and the frequency of temporal sampling τ . The spatial frequency describes the inverse distance between the fixed observation stations. The temporal frequency gives the rate at which new observations are read. The Model does not make use of measurements, the KF makes use of observations as they become available, the DLF uses observations as they become available as well as observations that are updated in time and space.

4.0.1. Example Problems

The model problems are chosen because they have analytical solutions. The Exact analytical solutions are linearly interpolated on the X to produce a solution we denote as *Truth*.

Problem I:

$$dx = -\alpha x dt + \beta dW,$$

with known initial conditions (initial probability density). In this case the relative drift is the constant $-\alpha$ and the variance of the incremental Wiener process dW is β . (In physical applications the constant $\alpha > 0$, where $1/\alpha$ is a commonly referred to as the relaxation time). The solution is

$$x_{n+1} = x_n e^{-\alpha \Delta t} + \left[\frac{\beta^2}{2\alpha} (1 - e^{-2\alpha \Delta t}) \right]^{1/2} \mathcal{N}(0, 1),$$

for $n = 0, 1, \dots, N_f - 1$. An approximate solution is given by

$$x_{n+1} = x_n - \alpha x_n \Delta t + \sqrt{\beta^2 \Delta t} \mathcal{N}(0, 1).$$

The mean and the variance of the solution are, respectively,

$$\langle x_{n+1} \rangle = \langle x_n \rangle e^{-\alpha \Delta t}, \quad \text{cov}(x_{n+1}) = \text{cov}(x_n) + \frac{\beta^2}{2\alpha} (1 - e^{-2\alpha \Delta t}) \beta = 0.02.$$

Problem II:

$$dx = (\alpha_0 + \alpha_1 t^{1/2}) dt + \beta dW,$$

with known initial conditions. Here α_0 and α_1 are constants. Problem B has a solution

$$x_{n+1} = x_n + \alpha_0 \Delta t + \frac{2}{3} \alpha_1 \Delta t^{3/2} + \sqrt{\beta^2 \Delta t} \mathcal{N}(0, 1),$$

for $n = 0, 1, \dots, N_f - 1$. $\mathcal{N}(0, 1)$ is a normal variate with variance 1. The mean and the covariance of the solution are, respectively,

$$\langle x_{n+1} \rangle = \langle x_n \rangle + \alpha_0 \Delta t + \frac{2}{3} \alpha_1 \Delta t^{3/2}, \quad \text{cov}(x_{n+1}) = \text{cov}(x_n) + \beta^2 \Delta t.$$

4.0.2. The Model

The Lax-Friedrichs discretization (Iserles (2006)) of (1) is adopted as the Model. Clearly, there are better discretizations than the Lax-Friedrichs, but the point is that in practice we have a model, which by definition, is the working approximation of the Truth. The forcing will be set to zero in the illustrative calculations. The model, for $u(t_n, X) := U^n \approx V^n$ is

$$V^{n+1} = L^n V^n + \sqrt{\Delta t} \Delta w_n, \quad n = 0, 1, 2, \dots$$

with known $V^0 = \langle U^0 \rangle$ and variance, periodic, and

$$L^n = \frac{1}{2} (1 - \lambda_\ell^n) \delta_{\ell, \ell+1} + \frac{1}{2} (1 + \lambda_\ell^n) \delta_{\ell, \ell-1},$$

for $\ell = 2, \dots, M - 1$, with periodized entries in the first and last rows:

$$\begin{aligned} L_{1,2}^n &= \frac{1}{2} (1 - \lambda_1^n) & L_{1,M}^n &= \frac{1}{2} (1 + \lambda_1^n) \\ L_{M,1}^n &= \frac{1}{2} (1 - \lambda_1^n) & L_{M,M-1}^n &= \frac{1}{2} (1 + \lambda_1^n) \end{aligned}$$

where

$$\lambda_\ell^n = \frac{\Delta t}{\Delta x} c(x_\ell, t_n).$$

The Courant-Friedrichs-Lewy condition (CFL) is set to 0.99. In the calculations that follow, once Δx is determined the Δt is determined via the wave speed and the CFL condition.

4.0.3. Fixed Parameters in the Examples

The discretization parameters will remain the same for every example shown. The domain has a length of $L = 2$, and it is discretized using $N = 50$ grid points in x , i.e., $\dim X = N = 50$ is the dimension of the state vector. In time there will be $N_f = 200$ time steps, for Problem I and $N_f = 100$ time steps, for Problem II. The initial condition is a pulse

$$U^0 = \frac{1}{S} [1 - 4(X - x_0)^2] \mathbb{I}_X + E,$$

where E is a normal variate vector with uncertainty $P_0 = 0.02$, and \mathbb{I}_X is a characteristic function. The normalization $S = \int_0^L [1 - 4(X - x_0)^2] \mathbb{I}_X dx$. For Example I, $x_0 = 1.25$ and for Example II, $x_0 = 1$. The forcing is purely stochastic: $f = 0$, $A = 0.01$. For Problem I: $\alpha_0 = 0.1$, $\alpha_1 = 0.01$. For Problem II: $\alpha = 0.01$. The variance of the observations is $R = 0.02$, and the variance of the model $Q = 4R$. The variance on the wave speed

4.0.4. Comparisons

Figures 2-4 summarize the outcomes for Problem I, with different filter sampling configurations. Figure 2 shows that the KF and the DLF are indistinguishable, and in very close agreement with an ensemble member of the Truth.

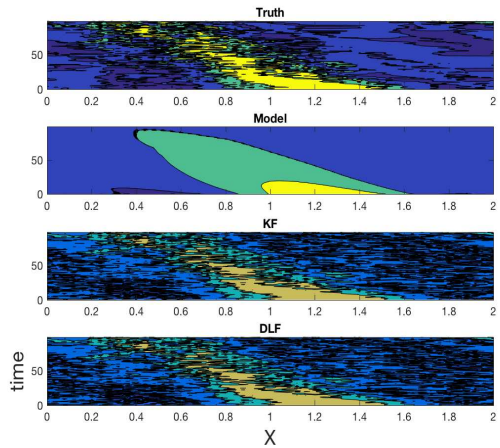


Figure 2. Problem I, Truth, Model, KF and DLF outcomes. New data is read at every time step (the temporal sampling frequency is $\tau = 1$) and at every spatial location (the spatial sampling frequency is $\xi = 1$).

Differences are noticed in the estimates when the filtering is done more sparsely. When the sampling is sparse, the DLF is qualitatively similar to the Truth, as compared to the KF outcome. This is shown in Figure 3

In Figure 4a the evolution of the center of mass of the different outcomes is compared, for sparse conditions. The Model estimate, as expected, diverges from the Truth estimate significantly, however, the KF or DLF are fairly close to each other and to the mean Truth. It is noted that, in this example problem over this short period of time, the Model provides a reasonably good estimate of the phase, when compared to the phase of the Truth. Hence, the KF and the DLF are given fairly good estimates in the prediction (forecasting) step. The uncertainty in the DLF is smaller than the KF but both of these are well within the expected bounds for the posterior uncertainty. See Figure 4b.

For Problem II, Figures 5-10 show the outcomes of an ensemble member of the Truth, the Model outcome, and the KF, and DLF outcomes. Figure 5 shows the space-time evolution corresponding to $\tau = 1/10$ and $\xi = 1$ case; Figure 6 to $\tau = 1$ and $\xi = 1/4$, and

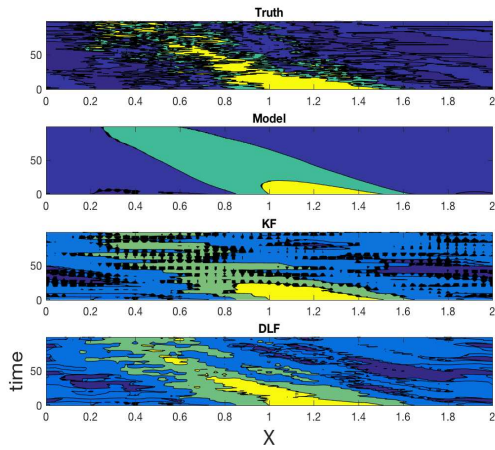


Figure 3. Problem I, Truth, Model, KF and DLF outcomes; $\tau = 1/10$ and $\xi = 1/5$.

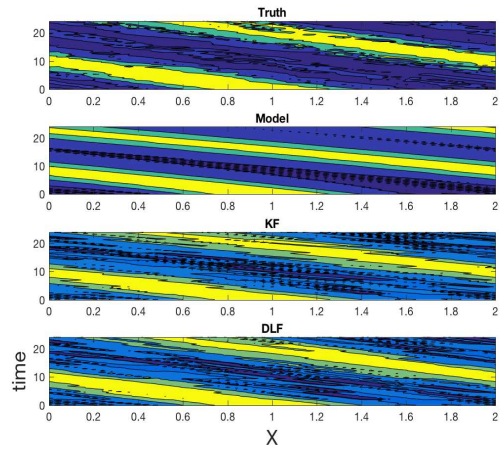
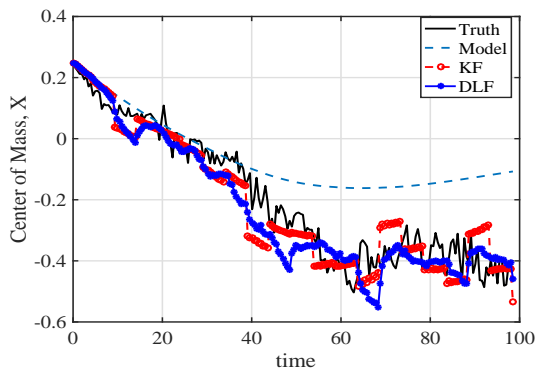
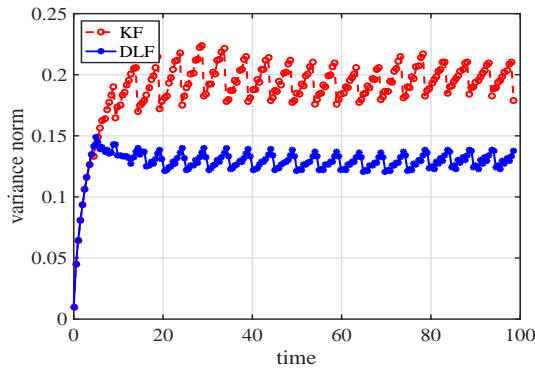


Figure 5. Problem II, Truth, Model, KF and DLF mean outcomes; $\tau = 1/10$, $\xi = 1$.



(a)



(b)

Figure 4. Problem I, Truth, Model, KF and DLF outcomes, (a) center of mass, (b) uncertainty; $\tau = 1/10$ and $\xi = 1/5$.

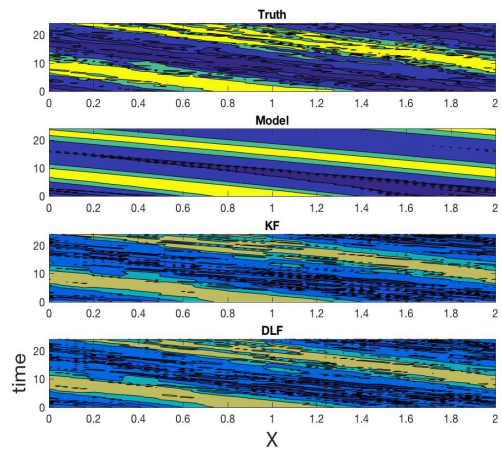


Figure 6. Problem II, Truth, Model, KF and DLF mean outcomes; $\tau = 1$, $\xi = 1/4$.

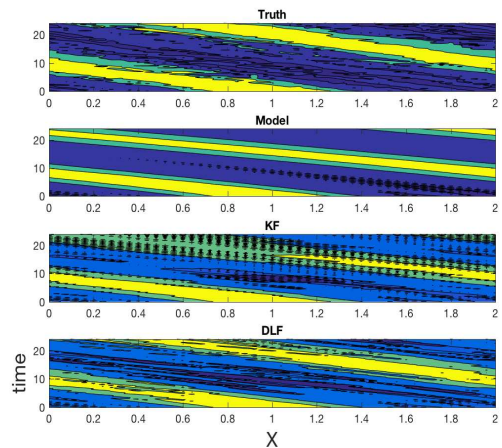


Figure 7. Problem II, Truth, Model, KF and DLF mean outcomes; $\tau = 1/10$, $\xi = 1/4$.

Figure 7 corresponds to $\tau = 1/10$ and $\xi = 1/4$, respectively. The DLF and the KF are comparable when the observation network is not sparse. Figure 8 shows the difference between an ensemble member of the Truth and the other three estimates, corresponding to the $\tau = 1/10$ and $\xi = 1/4$ case shown in Figure 7, suggesting a DLF estimate that is better than the KF estimate under sparse conditions. The DLF and the KF have superior phase outcomes, compared to the Model. The time evolution of the center of mass of the estimates and an ensemble member of Truth appear in Figure 9, for the parameters considered in Figures 5-8. The phase of the DLF is consistent with the Truth even when the observation system is sparse. Although the mean estimate provided by KF is not appreciably different from the DLF for the case when $\tau = 1$ and $\xi = 1/4$, the DLF has smaller uncertainties, as evidenced in Figure 10a. In Figure 10b, the uncertainties of the DLF and the KF estimates are compared. The KF uncertainty is running away.

5. Conclusions

A data assimilation, specifically tailored to advectively-dominated evolution partial different equations is proposed. When compared to a more traditional filtering scheme, the method is shown to improve estimated moments of the posterior distribution, composed of a likelihood informed by noisy observations, and a prior informed by noisy model outcomes, in cases where the observation network is sparse.

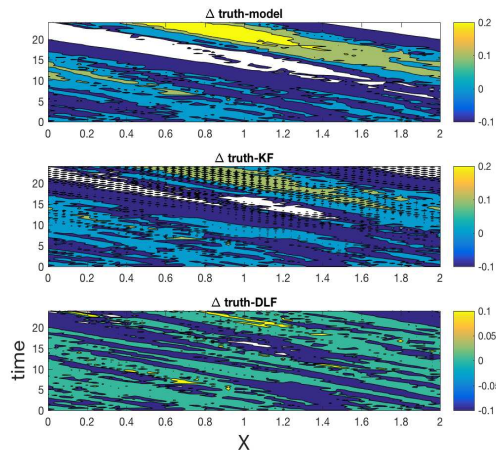


Figure 8. Problem II, difference between the Truth and the Model, the Truth and KF, and Truth and DLF; $\tau = 1/10$, $\xi = 1/4$.

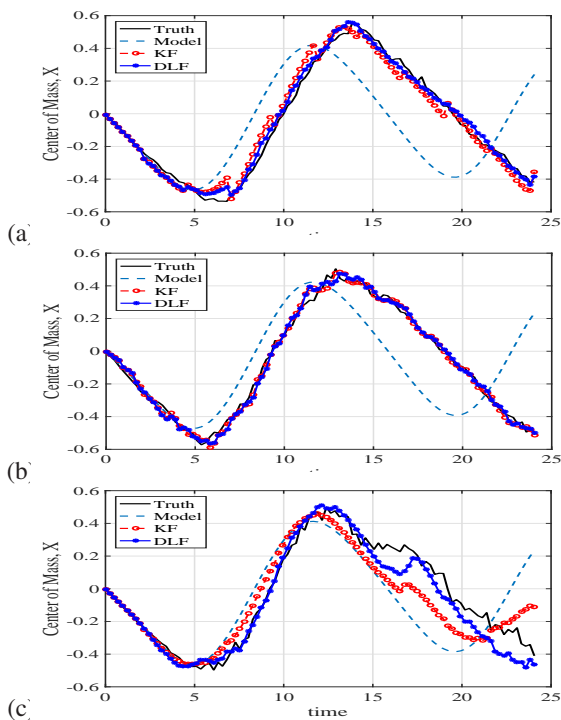


Figure 9. Problem II. Time evolution of the center of mass of the Truth, the Model, and the KF, and DLF estimates; (a) $\tau = 1/10$, $\xi = 1$, (b) $\tau = 1$, $\xi = 1/4$, and (c) $\tau = 1/10$, $\xi = 1/4$.

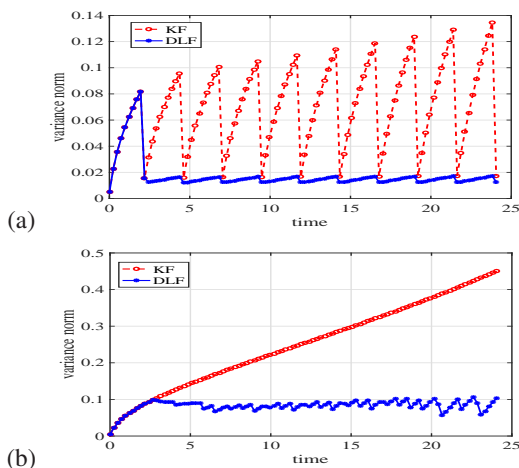


Figure 10. Problem II, uncertainty estimates for case (a) $\tau = 1/10$, $\xi = 1$, and (b) $\tau = 1/10$ and $\xi = 1/4$.

In advection-dominated dynamics, such as is the case in models of wave-like phenomena, dramatic improvements in forecasting can be made if the phase of the wave and the features of the field are well captured. Phase errors arise from epistemic errors and aleatoric errors in the phase speed. Both can affect features of the solution. Even if the physics are well captured by the model, the epistemic error in discrete models arises from truncation errors, which are usually deterministic. Aleatoric errors come from uncertainties in the wave speeds. These can also affect features of the wave, compounding errors in the wave due to amplitude uncertainties. The focus here was on the aleatoric error, since truncation errors are practically handled by making choices on the discretization of the physics model, rather than by filtering. (Obviously, epistemic and aleatoric errors also arise in the boundary conditions and in the initial conditions. Epistemic errors in the boundary/initial data can lead to bias errors in the estimate as well. Consideration of this source of error is not discussed in this study, however, the aleatoric initial condition error was accounted for, in a manner that is already standard in linear filtering methods. Gilling and Moor (2007), for example, considers the implication of some forms of epistemic error and their impact on filter estimates).

Data assimilation can lead to significant improvements in dynamic estimates, when observations with low uncertainty are blended. However, it is often the case in spatially-extended problems in geoscience that the observation system is sparse. This is particularly challenging in problems with 3 space dimensions and time (e.g., climate and weather models, solid mechanics, hydrology, etc). Moreover, with the higher resolutions afforded by larger computers the number of degrees of freedom in general is expected to grow by N^3 , a rate of growth that is impractical in observation systems. The trend is instead to decrease the uncertainty in the observation system. Sparse and low uncertainty observations pose a variety of challenges to filtering schemes, even if the biases from models and observations are properly accounted for; namely, the challenges of sampling very improbable events, and in hyperbolic and advection-dominated problems, in introducing phase errors in the estimates.

The proposed filtering technique, the *Dynamic Likelihood Filter* (DLF), is formulated to address phase and feature errors in the estimates in advection-dominated problems, when the observation system is sparse and of low uncertainty. It recasts the Bayesian statement that leads to a posterior distribution of the state variable, conditioned on observations, by exploiting the hyperbolic nature of the problem to propagate measurements forward in time. This adds a computational expense. However, since it is linear in the number of observation stations can be argued that in practical circumstances the added computational expense associated with using the deterministic time integrator to update at most N observations and their uncertainties is a reasonable price to pay, especially if the number of spatial dimensions reaches 3 (and thus the number of degrees of freedom, $\mathcal{O}(N^3)$).

For a simple linear hyperbolic system, the DLF delivered estimates that were superior to the KF, for sparse and high quality data. It was also shown that the data assimilation yielded estimates that were superior than estimates obtained with model-only predictions.

It is envisioned that there would be two variants of the Dynamic Likelihood Filter. When the measurements are fixed in space, which is the situation that was examined in this study, and a Lagrangian variant, in which the measurements are taken by a moving passive or active observational platforms. For the fixed observation network case there are some obvious directions to pursue in future work on dynamic likelihood filtering: in addition to generalizing to higher physical spatial dimensions,

the nonlinear/non-Gaussian data assimilation problems needs to be addressed. The present work focused on the fixed dynamic likelihood as it applies to the simplest possible hyperbolic problem. Namely, a linear one-way wave equation with uncertainties in the wave speed. Since the problem is linear and Gaussian, a Kalman filter scheme was used. The smoother can be obtained by variational methods, most naturally, by the representer method (*cf.*, Mead and Bennett (2001), and Bennett (2002)) for the hyperbolic dynamics case. Other issues that could be pursued in future are: (1) how to blend data and models when several observations inform a single state variable, which is in fact a challenge for many other filtering schemes; (2) in DLF, how best to interpolate data in the multi-analysis stage; (3) exploring DLF forecasts, in which the influence of data is projected forward in time with the goal of using it to improve forecasts of future states via the Bayesian methodology.

Acknowledgement

This work was supported by PEER research grant #1123-NCTRYH, and NSF/OCE #1434198. I wish to thank Stockholm University Rossby Fellowship Program, and MPE at Imperial College, London, for their hospitality.

References

- Ades M, VanLeeuwen PJ. 2015. The equivalent-weights particle filter in a high-dimensional system. *Quarterly Journal of the Royal Meteorological Society* **141**: 4845-503.
- Alexander FJ, Eyink GL, Restrepo JM. 2005. Accelerated Monte-Carlo for optimal estimation of time series. *Journal of Statistical Physics* **119**: 1331–1345.
- Bennett A. 2002. *Inverse modeling of the ocean and atmosphere*. Cambridge University Press: Cambridge, UK.
- Chorin A, Morzfeld M, Tu X. 2010. Implicit particle filters for data assimilation. *Communications in Applied Mathematics and Computational Science* **5**: 221–240.
- Courtier P, Derber J, Errico R, Louis JF, Vukicevic T. 1993. Important literature on the use of adjoint, variational methods and the Kalman filter in meteorology. *Tellus* **45A**: 342–357.
- Evensen G. 2003. The Ensemble Kalman Filter: theoretical formulation and practical implementation. *Ocean Dynamics* **53**: 343–367.
- Evensen G. 2004. Sampling strategies and square root analysis schemes for the EnKF. *Ocean Dynamics* **54**: 539–560.
- Eyink GL, Restrepo JM, Alexander FJ. 2004. A mean field approximation in data assimilation for nonlinear dynamics. *Physica D* **194**: 347–368.
- Gilling S, Moor BD. 2007. Model error estimation in ensemble data assimilation. *Nonlinear Processes in Geophysics* **14**: 59–71.
- Hamill TM, Snyder C. 2000. A hybrid ensemble Kalman filter 3D variational analysis scheme. *Monthly Weather Review* **128**: 2905–2919.
- Hoke J, Anthes RA. 1976. The initialization of numerical models by a dynamic initialization technique. *Monthly Weather Review* **104**: 1551–1556.
- Iserles A. 2006. *A first course in the numerical analysis of differential equations*. Cambridge University Press: Cambridge.
- Jazwinski AH. 1970. *Stochastic processes and filtering theory*, vol. 63. Academic Press.
- Kim S, Eyink GL, Restrepo JM, Alexander FJ, Johnson G. 2003. Ensemble filtering for nonlinear dynamics. *Monthly Weather Review* **131**: 2586–2594.
- Krause P, Restrepo JM. 2009. Lagrangian data assimilation using the Kernel Diffusion Method. *Monthly Weather Review* **137**: 4386–4400.
- Kushner HJ. 1962. On the differential equations satisfied by conditional probability densities of Markov processes, with applications. *SIAM Journal on Control, Series A* **2**: 106–119.
- Kushner HJ. 1967a. Approximation to optimal nonlinear filters. *IEEE Transactions on Automatic Control* **12**: 546–556.
- Kushner HJ. 1967b. Dynamical equations for optimal nonlinear filtering. *Journal of Differential Equations* **3**: 179–190.
- Kuznetsov L, Ide K, Jones C. 2003. A method for assimilation of Lagrangian data. *Monthly Weather Review* **131**: 2247–2260.
- Lorenz AC, Hammon O. 1988. Objective quality control of observations using bayesian methods. theory, and a practical implementation. *Q. J. R. Meteorol. Soc.* **114**: 515–543.
- Mead, Bennett AF. 2001. Towards regional assimilation of Lagrangian data: the Lagrangian form of the shallow water model and its inverse. *Journal of Marine Sciences* **29**: 365–384.
- Nehrkorn T, Woods B, Hoggman RN, Auligne T. 2015. Correcting for position errors in variational data assimilation. *Monthly Weather Review* **143**: 1368–1381.
- Ravela S. 2012. Quantifying uncertainty of coherent structures. *Procedia Computer Science* **9**: 1187–1196.
- Restrepo JM. 2008. A path integral method for data assimilation. *Physica D* **237**: 14–27.
- Rosenthal S, Venkataramani S, Mariano A, Restrepo JM. 2016. Displacement data assimilation. *Journal of Computational Physics* .
- Staniforth A, Coté J. 1991. Semi-lagrangian schemes for atmospheric models - a review. *Monthly Weather Review* **119**: 2206–2223.
- Stuart A, Voss J, Wiberg P. 2004. Conditional path sampling of SDEs and the Langevin MCMC method. *Communications in the Mathematical Sciences* **2**: 685–697.
- Weare J, Vanden-Eijnden E. 2013. Data assimilation in the low noise regime with applications to the Kuroshio. *Monthly Weather Review* **141**: 1822–1841.
- Wunsch C. 1996. *The ocean circulation inverse problem*. Cambridge University Press: Cambridge, UK.